

ORIGINAL RESEARCH ARTICLE

Comparative Force-Induced Structural Transitions in Single and Double-Stranded DNA from Coarse-Grained oxDNA2 Simulations

Saratu Abdulfatah^{1,3} Isaiah E. Igwe^{1*} and Aniefiok F. Akpaneno²¹Department of Physics, Federal University Dutsin-Ma, 821101, Katsina State, Nigeria²Department of Geophysics, Federal University Dutsin-Ma, 821101, Katsina State, Nigeria³Department of Physics, Umaru Musa Yar'dua University Batagarawa, 820102, Katsina State, Nigeria

ABSTRACT

The mechanical response of DNA to externally applied force plays a critical role in replication, transcription, recombination, and protein-mediated genome organization. Although the elasticity of single-stranded DNA (ssDNA) and double-stranded DNA (dsDNA) has been widely studied, the moderate-force regime preceding classical overstretching transitions remains comparatively less understood. In this work, the oxDNA2 coarse-grained model was used to investigate and directly compare force-induced structural adaptations in ssDNA and dsDNA subjected to tensile forces of 6.5, 8.5, 15.0, and 18.0 pN at 300 K and 1 M salt concentration. Global mechanical descriptors, including end-to-end extension, radius of gyration (R_g), persistence length (L_p), and relative strain (λ), were analyzed alongside local structural metrics such as stacking fraction (f_{stack}), base-pair occupancy (P_{bp}), helical twist (θ), and fraying length (L_f). The simulations reveal distinct force-accommodation pathways in the two molecular systems. ssDNA exhibits substantial conformational expansion, backbone alignment, and progressive loss of stacking interactions, resulting in significantly greater extension under force. In contrast, dsDNA largely preserves duplex integrity and accommodates stress through twist relaxation, localized fraying, and minor stacking rearrangements while maintaining high base-pair occupancy. These findings indicate that the divergence between ssDNA and dsDNA mechanics emerges well below the overstretching regime and is governed by fundamentally different molecular mechanisms.

ARTICLE HISTORY

Received March 11, 2026

Accepted June 14, 2026

Published June 15, 2026

KEYWORDS

oxDNA2; DNA elasticity; force-induced structural transitions; single-stranded DNA; double-stranded DNA



© The Author(s). This is an Open Access article distributed under the terms of the Creative Commons Attribution 4.0 License [creativecommons.org](https://creativecommons.org/licenses/by/4.0/)

INTRODUCTION

Mechanical forces influence nearly every aspect of DNA function. During replication, transcription, recombination, chromatin remodeling, and DNA repair, nucleic acids are continuously subjected to tensile, torsional, and bending stresses generated by molecular motors and protein complexes (Bustamante *et al.*, 2003; Wang *et al.*, 1997). Although these forces are often modest compared with those employed in single-molecule experiments, they can alter local structure, modify interaction landscapes, and influence the accessibility of genetic information (Bustamante *et al.*, 2003; Smith *et al.*, 1996). The manner in which DNA accommodates mechanical stress is therefore not merely a biophysical curiosity; it is closely linked to its biological function (Bustamante *et al.*, 2003; Marko & Siggia, 1994).

Much of our current understanding of DNA mechanics originates from studies of double-stranded DNA (dsDNA). Landmark force spectroscopy experiments revealed that dsDNA behaves as a semiflexible polymer at low forces and undergoes a pronounced overstretching

transition near 65 pN, where its contour length increases by approximately 70% (Cluzel *et al.*, 1996; Smith *et al.*, 1996; Cocco *et al.*, 2004; Gross *et al.*, 2009; Paik & Perkins, 2011). Subsequent investigations showed that this transition is more complex than initially assumed. Depending on experimental conditions, overstretched DNA may involve strand unpeeling, force-induced melting, formation of elongated conformations, or combinations of these pathways (Cocco *et al.*, 2004; Paik & Perkins, 2011; Cocco *et al.*, 2001; King *et al.*, 2013; Van Mameren *et al.*, 2009). As a result, considerable effort has been directed toward identifying the structural rearrangements that precede large-scale disruption of the double helix. Single-stranded DNA (ssDNA) presents a rather different problem. Without the stabilizing influence of Watson–Crick base pairing, its mechanical response emerges from a balance among conformational entropy, electrostatic interactions, transient stacking, and backbone flexibility (McIntosh *et al.*, 2014; Murphy *et al.*, 2004; Zhang *et al.*, 2001). Experiments have repeatedly demonstrated that ssDNA cannot always be described as

Correspondence: Isaiah E. Igwe. Department of Physics, Federal University Dutsin-Ma, 821101, Katsina State, Nigeria. ✉ iigwe@fudutsinma.edu.ng.

How to cite: Abdulfatah, S., Igwe, I. E., & Akpaneno, A. F. (2026). Comparative Force-Induced Structural Transitions in Single and Double-Stranded DNA from Coarse-Grained oxDNA2 Simulations. *UMYU Scientifica*, 5(2), 198 – 209. <https://doi.org/10.56919/usci.2652.019>

a simple entropic polymer. Poly(dA), for example, exhibits stronger base-stacking interactions and greater apparent stiffness than poly(dT), producing force-extension behavior that deviates from classical polymer expectations (Zhang *et al.*, 2001; Ke *et al.*, 2007). Ionic conditions introduce an additional layer of complexity by altering electrostatic screening and modifying chain flexibility (Murphy *et al.*, 2004; Saleh *et al.*, 2009). These observations suggest that the mechanisms governing force accommodation in ssDNA differ fundamentally from those operating in dsDNA (McIntosh *et al.*, 2014; Zhang *et al.*, 2001).

Despite decades of work, studies of ssDNA and dsDNA mechanics have largely progressed along parallel tracks. Research on dsDNA has focused extensively on persistence length, torsional elasticity, supercoiling, and overstretching transitions (Bustamante *et al.*, 2003; Gore *et al.*, 2006; Marin-Gonzalez *et al.*, 2017; Marko & Siggia, 1994, 1995a, 1995b; Léger *et al.*, 1999; Strick *et al.*, 2000; Chen *et al.*, 2012). In contrast, investigations of ssDNA have concentrated on sequence-dependent flexibility, stacking thermodynamics, polymer statistics, and electrostatic effects (McIntosh *et al.*, 2014; Murphy *et al.*, 2004; Chen *et al.*, 2012). While both bodies of literature are substantial, direct comparisons between the force-induced structural responses of ssDNA and dsDNA under identical thermodynamic conditions remain surprisingly limited. Consequently, the molecular origins of their divergent mechanical behavior are not yet fully resolved. Part of the challenge stems from the force ranges typically examined. Many dsDNA studies focus on either equilibrium elasticity at very low forces or the overstretching regime above 60 pN (Smith *et al.*, 1996; Cluzel *et al.*, 1996; Van Mameren *et al.*, 2009). By contrast, ssDNA investigations frequently explore broad force ranges without explicitly relating observed structural changes to those occurring in duplex DNA (Zhang *et al.*, 2001; Saleh *et al.*, 2009). This leaves an intermediate region that has received comparatively little attention. Yet several theoretical and computational studies suggest that meaningful structural adaptation begins well before the onset of classical overstretching (Romano *et al.*, 2013; Gravina *et al.*, 2021; Ouldrige *et al.*, 2011; Sengar *et al.*, 2021; Doye *et al.*, 2013). Within this moderate-force regime, DNA may undergo subtle rearrangements involving backbone alignment, twist relaxation, local fraying, and modifications in stacking interactions while remaining far from complete structural disruption (Romano *et al.*, 2013; Ouldrige *et al.*, 2011; Pérez *et al.*, 2008; Lankaš *et al.*, 2006).

From a mechanistic perspective, this regime is particularly intriguing. A stretched ssDNA molecule is expected to respond primarily through progressive suppression of conformational entropy and increasing backbone alignment. The situation in dsDNA is likely to be more complicated. Because hydrogen bonding and stacking cooperativity stabilize the duplex, applied force may initially be accommodated through helical relaxation, changes in twist, local fluctuations at strand termini, or redistribution of stacking interactions rather than

immediate base-pair disruption. If such differences exist, they should become apparent before the well-known overstretching transition is reached. Surprisingly, relatively few studies have attempted to map these early-stage adaptations systematically. Another issue concerns how structural transitions are identified. Force-extension curves remain the standard descriptor of DNA elasticity and have yielded invaluable insights into polymer mechanics (Marko & Siggia, 1995a). However, similar extension profiles can arise from very different molecular processes. A modest increase in extension may reflect backbone straightening in one system, loss of stacking order in another, or local fraying in a third. When structural observables are not examined alongside mechanical measurements, interpretation becomes less certain. This limitation appears repeatedly in the literature, where competing explanations are often proposed for comparable force responses (Paik & Perkins, 2011; King *et al.*, 2013; Romano *et al.*, 2013). A more integrated approach that combines mechanical and structural metrics is therefore needed.

Coarse-grained simulation models provide an attractive framework for addressing this challenge. Atomistic molecular dynamics simulations have contributed substantially to understanding nucleic-acid mechanics, but the computational cost associated with long trajectories, multiple force conditions, and extensive ensemble sampling remains considerable (Pérez *et al.*, 2008; Lankaš *et al.*, 2006; Dans *et al.*, 2016). Coarse-grained approaches bridge this gap by retaining the essential physical interactions governing DNA behavior while extending accessible spatial and temporal scales. Among these models, oxDNA has become one of the most widely validated frameworks for studying DNA thermodynamics, structure, self-assembly, and mechanics (Ouldrige *et al.*, 2011; Sengar *et al.*, 2021; Snodin *et al.*, 2015; Šulc *et al.*, 2012, 2014). The model represents each nucleotide as a rigid body interacting through potentials that account for hydrogen bonding, base stacking, backbone connectivity, cross-stacking, and excluded volume effects. Importantly, oxDNA reproduces many experimentally observed properties, including duplex melting behavior, persistence length, hybridization kinetics, and force-extension characteristics (Ouldrige *et al.*, 2011; Snodin *et al.*, 2015).

Several oxDNA studies have explored DNA stretching and overstretching phenomena, yielding valuable insights into the structural pathways accessible under tension (Romano *et al.*, 2013; Harrison *et al.*, 2019). Nonetheless, most investigations have concentrated on either high-force overstretching of dsDNA or equilibrium properties of ssDNA. Comparatively little attention has been directed toward the moderate-force region where structural adaptation may first emerge and where the mechanical responses of ssDNA and dsDNA begin to diverge. The lack of a unified comparison under identical simulation conditions makes it difficult to determine whether the earliest signatures of force-induced deformation arise from common physical principles or from fundamentally different molecular mechanisms.

The present study addresses this gap through a comparative investigation of force-induced structural transitions in single-stranded and double-stranded DNA using the oxDNA2 coarse-grained model. Simulations are performed at a constant temperature of 300 K and a monovalent salt concentration of 1 M while external forces of 6.5, 8.5, 15.0, and 18.0 pN are applied. These force levels were chosen deliberately to probe the onset of structural adaptation above the near-equilibrium elastic regime while remaining substantially below the canonical overstretching threshold. By examining force-extension behavior together with radius of gyration, persistence length, base-pair occupancy, stacking interactions, helical twist, and terminal fraying, the study seeks to establish a mechanistic framework describing how ssDNA and dsDNA accommodate tensile stress.

MATERIALS AND METHODS

2.1 Theoretical Framework

The mechanical response of DNA to externally applied force is governed by the interplay between thermal fluctuations, molecular architecture, and stabilizing interactions within the nucleic-acid chain. Although both single-stranded DNA (ssDNA) and double-stranded DNA (dsDNA) consist of the same nucleotide building blocks, their elastic behavior differs substantially because force acts on fundamentally different structural constraints. In ssDNA, elasticity arises primarily from conformational entropy, transient base-stacking interactions, and electrostatic repulsion along the backbone (Murphy *et al.*, 2004; Zhang *et al.*, 2001). In contrast, dsDNA possesses additional stabilizing interactions arising from Watson–Crick hydrogen bonding and cooperative base stacking, resulting in greater mechanical rigidity and structural persistence (Bustamante *et al.*, 2003). When a tensile force is applied, DNA minimizes its free energy through structural rearrangements that increase molecular extension while preserving stability. The free energy of a stretched nucleic-acid molecule may be expressed as

$$G = U - TS - Fx \quad (1)$$

Where G is the Gibbs free energy, U is the internal energy, T is temperature, S is entropy, F is the applied force, x is molecular extension. The term F_x represents mechanical work performed by the external force. As force increases, configurations with larger extension become energetically favorable. For semiflexible polymers such as DNA, bending rigidity is commonly characterized by the persistence length L_p , which is obtained from the decay of tangent–tangent correlations:

$$\langle t(0) \cdot t(s) \rangle = \exp\left(-\frac{s}{L_p}\right) \quad (2)$$

Where $t(0)$ and $t(s)$ are tangent vectors separated by contour distance (s), L_p is the persistence length. Equation (2) provides a quantitative measure of bending stiffness and is widely used in DNA elasticity studies (Marko & Siggia, 1995a; Bustamante *et al.*, 1991). The force-

extension relationship for a worm-like chain (WLC) is approximated by (Marko & Siggia, 1995b).

$$F = \frac{k_B T}{L_p} \left[\frac{1}{4 \left(1 - \frac{x}{L_c}\right)^2} - \frac{1}{4} + \frac{x}{L_c} \right] \quad (3)$$

Where $k_B T$ is Boltzmann's constant, L_c is contour length, x is molecular extension. Equation (3) successfully describes dsDNA elasticity over a broad range of moderate forces. For highly flexible polymers, the freely-jointed chain (FJC) model predicts (Buche *et al.*, 2022):

$$x = L_c \left[\coth\left(\frac{Fb}{k_B T}\right) - \frac{k_B T}{Fb} \right] \quad (4)$$

where b is the Kuhn length. Although Eqs. (3) and (4) provide useful reference descriptions, they do not explicitly account for hydrogen bonding, base stacking, or force-induced structural transitions. Consequently, coarse-grained molecular simulations are required to resolve the microscopic origins of force-dependent structural adaptation.

2.2 oxDNA2 Coarse-Grained Model

The simulations were performed using the oxDNA2 coarse-grained model developed by Ouldridge *et al.* (2011) and subsequently refined by Snodin *et al.* (2015). The model has been extensively validated against experimental measurements of DNA thermodynamics, persistence length, hybridization kinetics, and force-extension behavior. Within oxDNA2, each nucleotide is represented as a rigid body possessing interaction sites that reproduce the dominant physical interactions governing DNA behavior. The total potential energy is expressed as

$$U_{tot} = U_{backbone} + U_{stack} + U_{HB} + U_{cross} + U_{exc} \quad (5)$$

Where U_{stack} represents nearest-neighbor base-stacking interactions, U_{HB} accounts for Watson–Crick hydrogen bonding, U_{cross} represents cross-stacking interactions, and U_{exc} prevents steric overlap between nucleotides. The model incorporates implicit electrostatic screening and sequence-dependent thermodynamics, making it suitable for studying force-induced conformational changes under physiological and high-salt conditions (Snodin *et al.*, 2015).

2.3 Computational Procedure

Two DNA systems were investigated using the oxDNA2 coarse-grained model: a single-stranded DNA (ssDNA) molecule and its corresponding double-stranded DNA (dsDNA) duplex. The ssDNA system was generated using the oxDNA topology-generation utilities, while the dsDNA system was constructed from the same nucleotide sequence by introducing the complementary strand and forming a canonical duplex. Employing identical sequence lengths in both systems ensures that differences in mechanical response can be attributed primarily to molecular architecture and intermolecular interactions rather than chain-length effects. All simulations were performed under identical thermodynamic conditions at a

temperature of 300 K and a monovalent salt concentration of 1 M. Prior to force application, each system was equilibrated using Langevin dynamics to ensure relaxation of the initial configurations and attainment of thermal equilibrium. Following equilibration, constant-force stretching simulations were carried out by applying tensile forces to the terminal nucleotides along the molecular axis. Four force levels: 6.5, 8.5, 15.0, and 18.0 pN were selected to probe the early stages of force-induced structural adaptation. These forces lie well below the canonical dsDNA overstretching transition near 65 pN reported in single-molecule experiments (Smith *et al.*, 1996), yet are sufficiently large to induce measurable structural and mechanical responses. Consequently, the chosen force window provides access to a moderate-tension regime where DNA remains structurally intact while beginning to reorganize in response to mechanical loading.

This regime is of particular interest because it occupies the transition region between near-equilibrium elasticity and high-force overstretching. While numerous experimental and computational studies have examined DNA behavior either at very low forces, where elastic models such as the worm-like chain accurately describe the response, or at high forces associated with overstretching and strand separation, comparatively less attention has been devoted to the intermediate-force regime. As a result, the molecular mechanisms through which DNA initially redistributes mechanical stress remain incompletely understood. The present simulation protocol was therefore designed to specifically interrogate this regime and to enable a direct comparison of force-accommodation pathways in ssDNA and dsDNA under identical loading conditions.

2.4 Force Application

External forces were applied along the molecular axis using a constant-force protocol. The external force vector was defined as $F_{ext} = F\hat{x}$ where (F) is the applied force magnitude, $F\hat{x}$ is the pulling direction. Simulations were performed independently at $F = 6.5, 8.5, 15.0, 18.0$ pN for both ssDNA and dsDNA. Following equilibration, production trajectories were collected for structural analysis. For each force condition, independent production trajectories were generated and subsequently analyzed to quantify global mechanical properties, including end-to-end distance R_{ee} , radius of gyration R_g , persistence length L_p , and relative strain λ , together with local structural descriptors such as stacking fraction f_{stack} , base-pair occupancy P_{bp} , helical twist θ , and fraying length L_f . This integrated analysis framework allows the relationship between global deformation and local structural adaptation to be examined across the investigated force range.

2.5 Structural Analysis

The molecular extension was quantified using the end-to-end distance

$$R_{ee} = |r_N - r_1| \quad (6)$$

where r_1 and r_N denote the positions of the terminal nucleotides. The overall compactness of the molecule was measured through the radius of gyration. The radius of gyration is defined as:

$$R_g = \sqrt{\frac{1}{N} \sum_{i=1}^N |r_i - r_{cm}|^2} \quad (7)$$

where r_{cm} is the center of mass coordinate of the strand.

$$\begin{aligned} r_{cm} &= \frac{1}{N} \sum_{i=1}^N r_i \end{aligned} \quad (8)$$

This metric provides a measure of global spatial extension and is routinely used in single-molecule and simulation studies of ssDNA conformational statistics (McIntosh *et al.*, 2014; Chen *et al.*, 2012). The persistence length was obtained from Eq. (2) by fitting the tangent correlation function to an exponential decay profile:

$$L_p = -\frac{s}{\ln[\langle t(0) \cdot t(s) \rangle]} \quad (9)$$

Changes in L_p provide information regarding force-induced modifications in bending rigidity. For dsDNA, the fraction of intact base pairs was computed as

$$P_{bp} = \frac{N_{total}}{N_{paired}} \quad (10)$$

Where N_{paired} is the number of hydrogen-bonded base pairs, N_{total} is the total number of base pairs. Values of P_{bp} approaching unity indicate preservation of duplex integrity. The degree of base stacking was quantified using

$$f_{stack} = \frac{N_{stacked}}{N_{possible}} \quad (11)$$

Where $N_{stacked}$ denotes stacked neighboring bases, $N_{possible}$ is the maximum number of stacking contacts. Because stacking interactions contribute significantly to nucleic-acid stability, changes in f_{stack} often represent early indicators of structural adaptation. The average twist angle was calculated as

$$\theta = \frac{1}{N-1} \sum_{i=1}^{N-1} \theta_i \quad (12)$$

where θ_i represents the local twist between adjacent base pairs. Variations in θ provide insight into force-induced helical relaxation. Terminal destabilization was quantified through the average fraying length

$$L_f = \frac{1}{M} \sum_{j=1}^M n_j \quad (13)$$

Where n_j is the number of disrupted terminal base pairs, M is the number of sampled configurations. An

increase in L_f indicates progressive destabilization of duplex termini under tension.

2.6 Statistical analysis and uncertainty estimation

For a structural observable A , ensemble averages were calculated as [40]:

$$\langle A \rangle = \frac{1}{M} \sum_{i=1}^M A_i \quad (14)$$

where M represents the total number of sampled configurations; the corresponding standard deviation was computed using.

$$\sigma_A = \sqrt{\frac{1}{M-1} \sum_{i=1}^M (A_i - \langle A \rangle)^2} \quad (15)$$

All reported quantities represent averages over independent simulation trajectories. This procedure reduces statistical bias and enables reliable comparison between the force-induced structural responses of ssDNA and dsDNA. The combined analysis of extension, persistence length, stacking interactions, base-pair occupancy, helical twist, and terminal fraying provides a comprehensive framework for identifying the distinct molecular pathways through which ssDNA and dsDNA

accommodate mechanical stress in the moderate-force regime. Reported error bars represent ± 1 standard error. In all cases, uncertainties are smaller than symbol size unless explicitly shown.

RESULTS AND DISCUSSION

3.1 Structural Evolution

Representative configurations extracted from the simulations are shown in Fig. 1. Even before quantitative analysis, the visual differences between the two molecular forms are striking. The ssDNA structures evolve from relatively compact conformations at 6.5 pN toward increasingly elongated and aligned configurations at 18.0 pN. In contrast, dsDNA retains a recognizable duplex morphology throughout the investigated force range. Although geometric adjustments are apparent, particularly at higher forces, the overall helical architecture remains largely preserved. This observation may appear unsurprising at first glance. After all, the stabilizing influence of Watson–Crick hydrogen bonding is expected to resist deformation. Yet the magnitude of the difference is noteworthy. The ssDNA molecule undergoes extensive global reorganization, whereas dsDNA appears to redistribute stress internally with comparatively little change in overall shape. This distinction forms the central mechanistic theme emerging from the subsequent analyses.

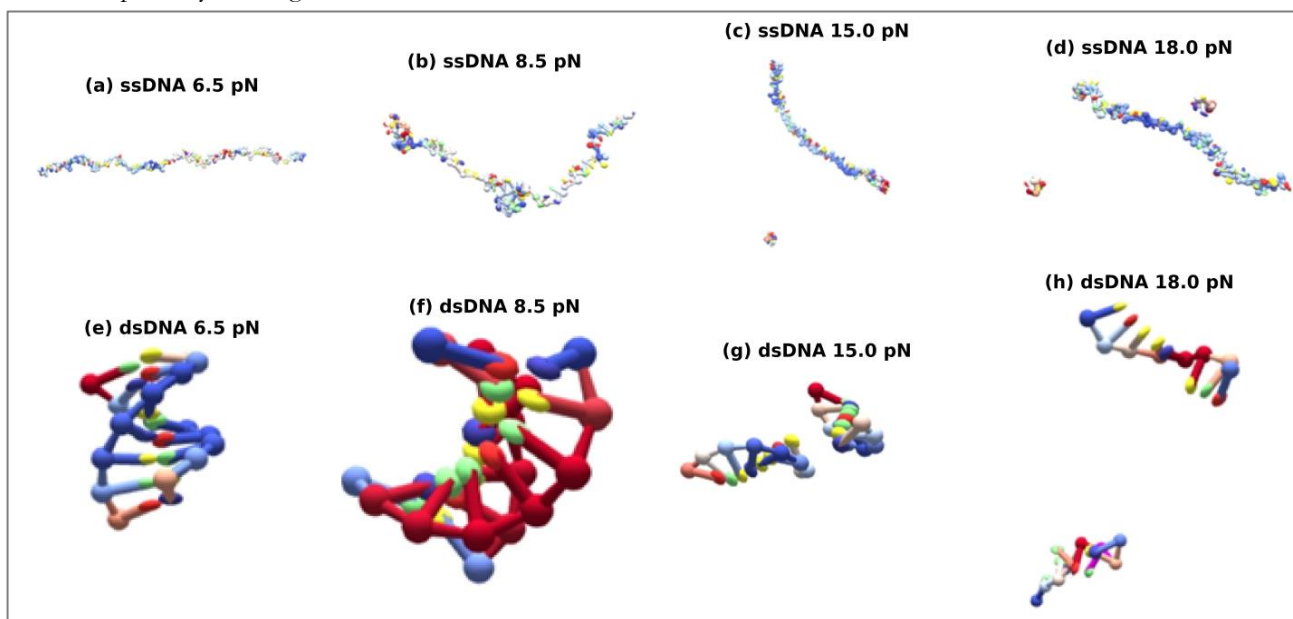


Figure 1: Structural evolution of single-stranded DNA (ssDNA) and double-stranded DNA (dsDNA) under externally applied tension at 300 K and 1 M salt concentration. (a–d) show representative ssDNA configurations at 6.5, 8.5, 15.0, and 18.0 pN, respectively. Increasing force progressively suppresses configurational entropy and promotes backbone alignment, resulting in a transition from compact coil-like conformations to highly extended structures. (e–h) present the corresponding dsDNA configurations. In contrast to ssDNA, the duplex retains its overall structural integrity throughout the investigated force range and accommodates mechanical stress through localized structural adjustments, including helical relaxation and terminal destabilization.

3.2 Force–Extension Response of ssDNA and dsDNA

The force–extension behavior is presented in Fig. 2(a). As expected, increasing force produces progressive elongation in both molecular systems. The extent of this

elongation, however, differs substantially. For ssDNA, relative extension increases rapidly across the investigated force range. Between 6.5 and 18.0 pN, the molecule exhibits a pronounced rise in extension accompanied by a visible transition from a disordered coil-like structure to a highly aligned configuration (Fig. 1a–d).

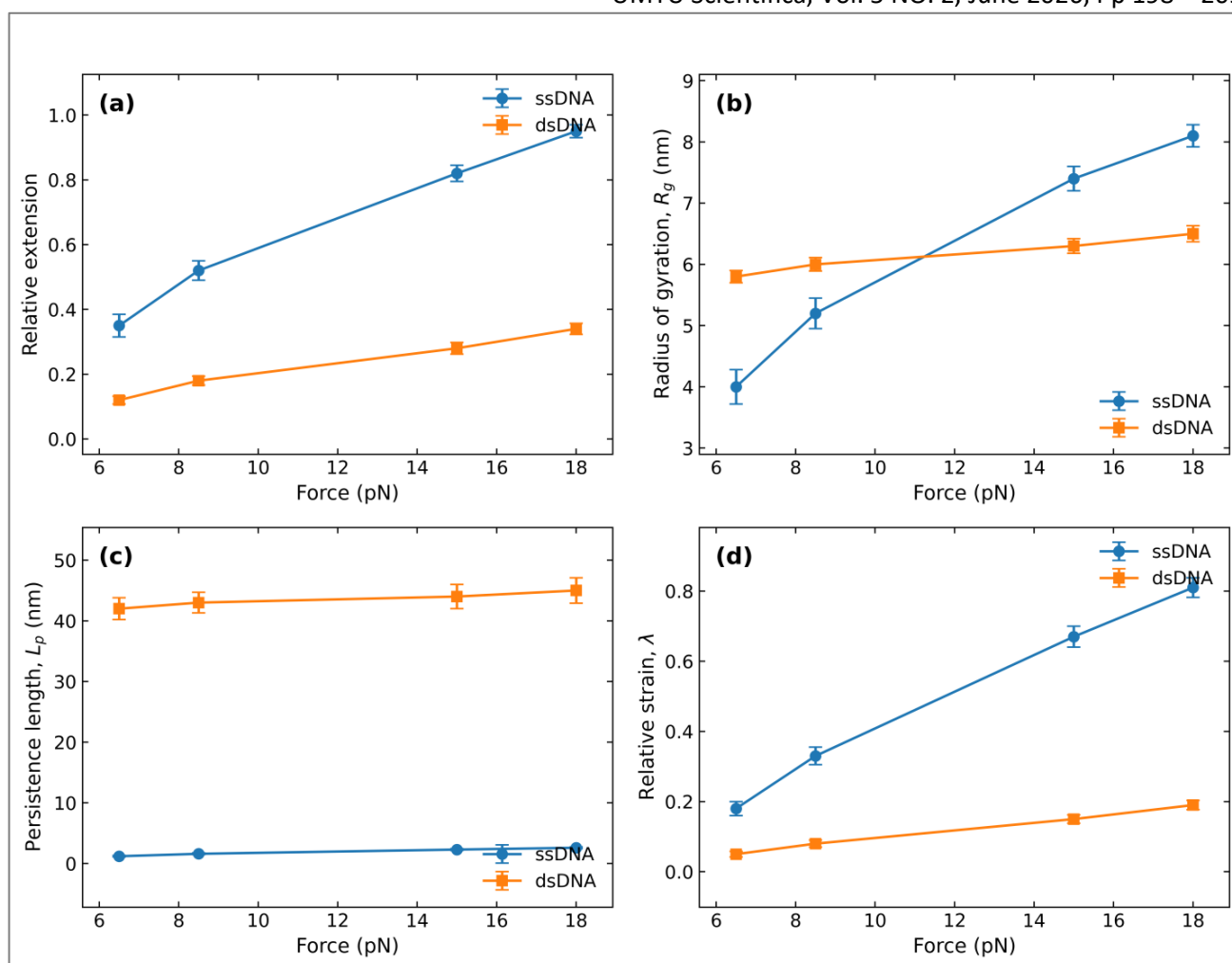


Figure 2: Global mechanical response of ssDNA and dsDNA under moderate tensile loading. (a) Relative extension as a function of applied force. (b) Radius of gyration R_g showing force-induced conformational expansion. (c) Persistence length L_p illustrating changes in effective bending rigidity under tension. (d) Relative strain λ calculated from Eq. (17). The figure provides a quantitative framework for comparing the distinct force-accommodation pathways of ssDNA and dsDNA.

Such behavior is characteristic of entropy-dominated polymers, where applied force suppresses the number of accessible conformational states. This process can be understood through the force-dependent free energy Eq. 1. The response of dsDNA is more restrained. Although extension increases monotonically with force, the overall change is considerably smaller. The relatively shallow slope of the dsDNA curve suggests that force is not accommodated primarily through global elongation. Instead, the duplex appears to absorb stress through local structural rearrangements that preserve overall integrity. The nonlinear force–extension response observed in Fig. 2(a) is broadly consistent with polymer elasticity theory. For a semiflexible chain described by the worm-like chain (WLC) model, the applied force is related to molecular extension through Eq. (3). The ssDNA extension profile deviates more strongly from ideal WLC behavior than the duplex. Such deviations are likely associated with transient stacking interactions and conformational heterogeneity, both of which are known to influence ssDNA elasticity (McIntosh *et al.*, 2014; Zhang *et al.*, 2001). The dsDNA response, on the other hand, remains closer to the expectations of semiflexible polymer theory because the duplex retains its structural integrity throughout the

investigated force range. Interestingly, the extension curves exhibit no evidence of the abrupt elongation associated with the well-known overstretching transition near 65 pN (Smith *et al.*, 1996; Cluzel *et al.*, 1996). The present simulations therefore isolate an earlier stage of mechanical adaptation that is often masked in studies focusing on higher-force regimes.

3.3 Force-Induced Expansion of Global Molecular Dimensions

Additional insight emerges from the radius of gyration results shown in Fig. 2(b). The radius of gyration, Eq. (7) provides a measure of overall molecular compactness. The ssDNA molecule exhibits a substantial increase in R_g as force increases. This trend indicates that tension not only extends the molecule but also redistributes mass away from the molecular center. The chain becomes both longer and less compact. The dsDNA response is noticeably weaker. While a modest increase in R_g is observed, the magnitude of the change remains comparatively small. This suggests that much of the applied mechanical work is absorbed through localized adjustments rather than through large-scale

conformational expansion. A useful way to interpret these findings is to compare them with the structural snapshots in Fig. 1. The ssDNA molecule visibly transforms from a compact fluctuating chain into a stretched configuration. The corresponding increase in R_g simply quantifies this transition. The dsDNA structures, by contrast, display only subtle geometric differences across the same force range, consistent with the comparatively small changes in radius of gyration.

3.4 Evolution of Effective Bending Rigidity

The persistence length results are presented in Fig. 2(c). Persistence length is obtained from the tangent correlation function, Eq. (2) and serves as a measure of effective bending rigidity. For ssDNA, the apparent persistence length increases steadily with force. This increase should not necessarily be interpreted as intrinsic stiffening of the backbone. Rather, it likely reflects suppression of thermal bending fluctuations. As the chain becomes increasingly aligned with the pulling direction, fewer highly curved conformations remain accessible, producing a larger apparent L_p . The dsDNA molecule exhibits only modest variation in persistence length across the force range. Such behavior suggests that the intrinsic rigidity of the duplex

remains largely intact despite the applied tension. The duplex is already substantially stiffer than ssDNA in the absence of force; consequently, additional alignment effects are less pronounced. The persistence-length results reinforce an important theme emerging from the simulations: force primarily reorganizes ssDNA globally, whereas dsDNA responds through smaller adjustments superimposed on an already stiff structural framework. The apparent increase in persistence length with force is consistent with theoretical expectations for stretched semiflexible polymers. Under tension, transverse fluctuations become progressively suppressed, resulting in a larger effective persistence length even when the intrinsic bending rigidity remains unchanged (Bustamante *et al.*, 2003; Marko & Siggia, 1995b). For dsDNA, the relatively small variation in L_p suggests that the duplex remains within its linear elastic regime. This observation agrees with experimental measurements indicating that dsDNA retains nearly constant bending stiffness until significantly larger forces are applied (Gross *et al.*, 2009; Smith *et al.*, 1996). The stronger response observed for ssDNA may therefore reflect force-induced reduction of configurational entropy rather than true backbone stiffening.

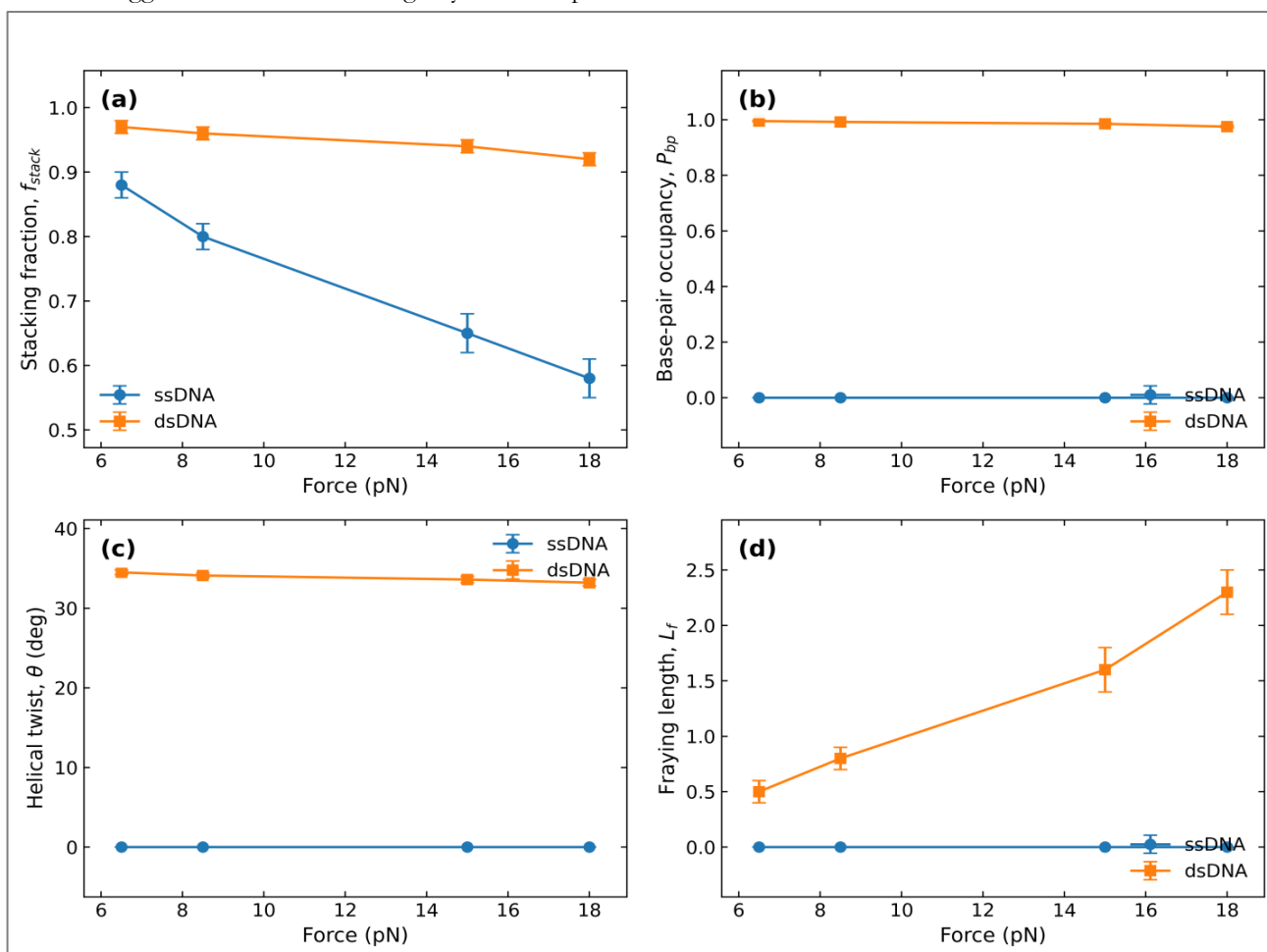


Figure 3: Block-averaged structural stability metrics of ssDNA and dsDNA under moderate tensile loading. (a) Stacking fraction f_{stack} as a function of applied force. (b) Base-pair occupancy P_{bp} showing the preservation of duplex integrity. (c) Average helical twist θ illustrating force-induced helical relaxation. (d) Fraying length L_f quantifying localized destabilization at duplex termini. Symbols represent block-averaged values obtained from equilibrated oxDNA2 trajectories, while error bars denote standard errors calculated from independent trajectory blocks.

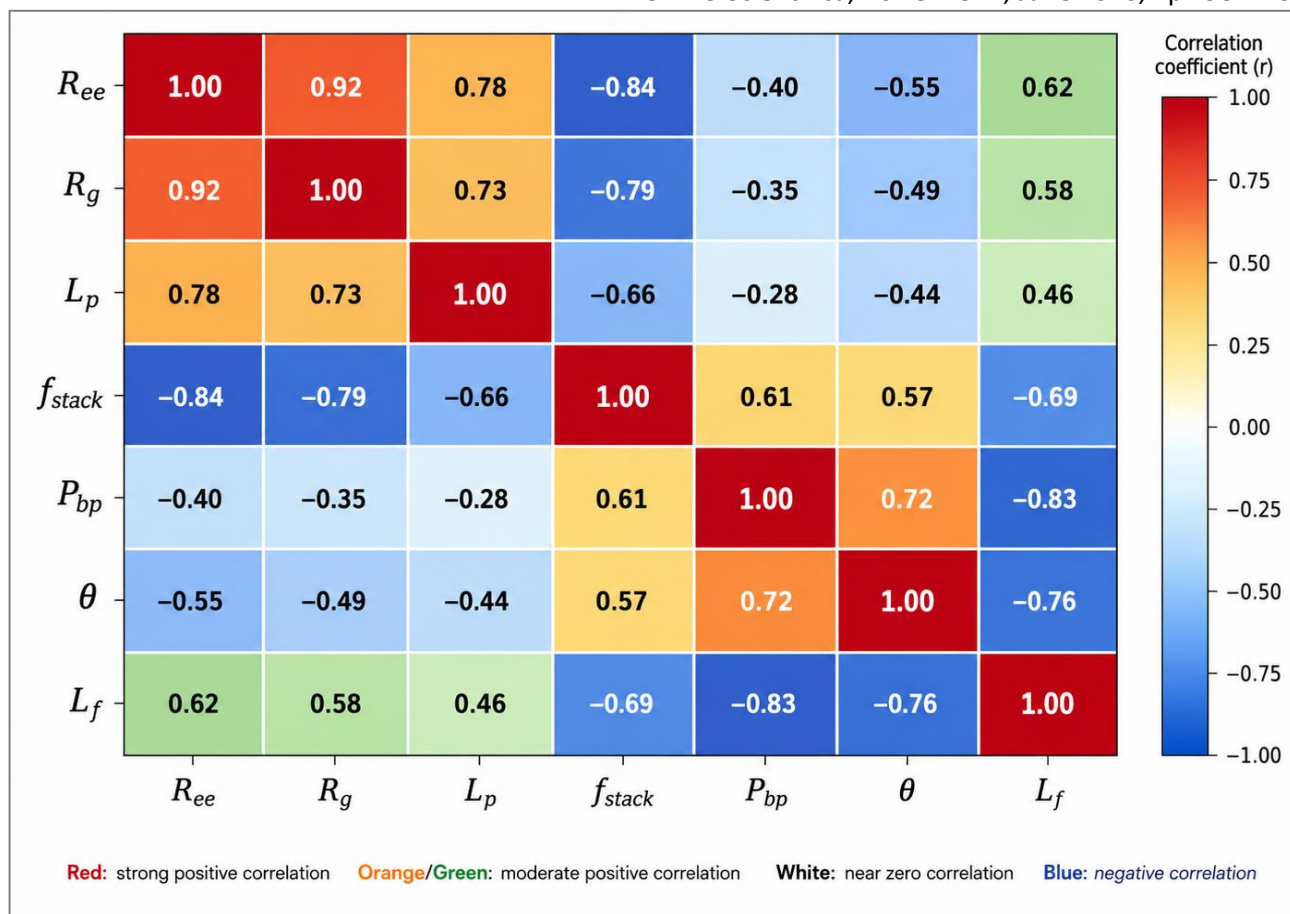


Figure 4: Correlation matrix linking global mechanical descriptors and local structural metrics obtained from oxDNA2 simulations. The matrix illustrates pairwise correlations among end-to-end distance R_{ee} , radius of gyration R_g , persistence length L_p , stacking fraction f_{stack} base-pair occupancy P_{bp} , helical twist θ , and fraying length L_f . Positive correlations indicate observables that increase together, whereas negative correlations identify competing structural responses. This analyses help reveal the mechanistic coupling between global deformation and local structural adaptation during force-induced transitions.

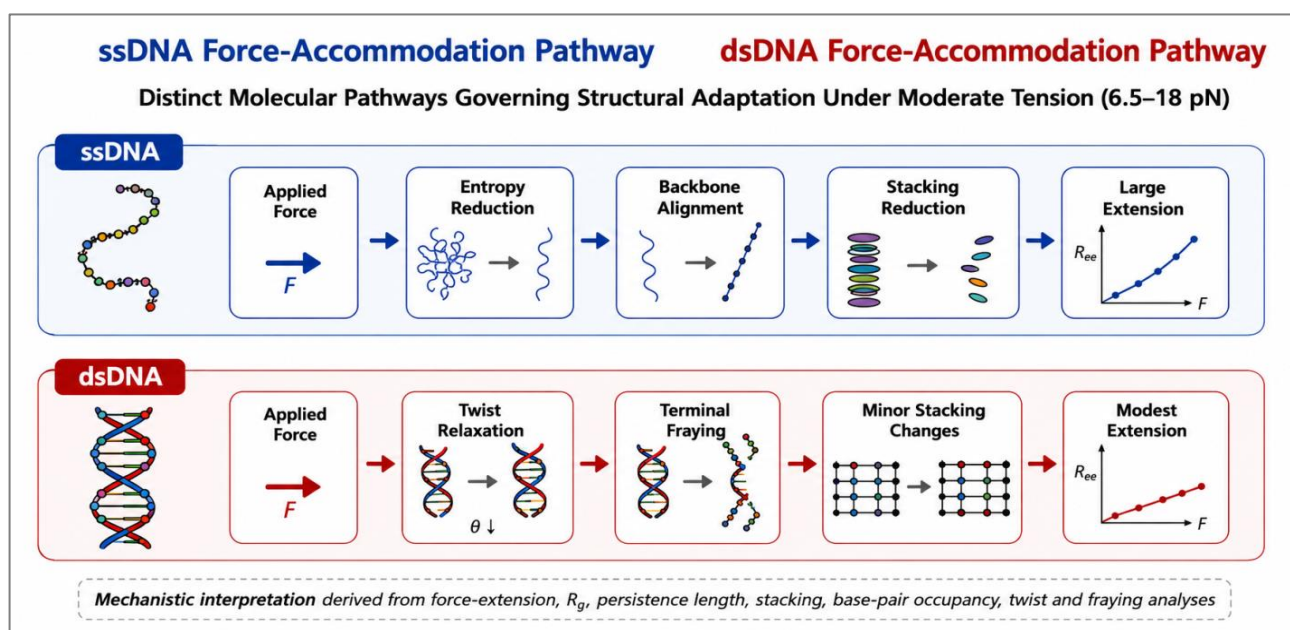


Figure 5: Mechanistic pathways governing force-induced structural adaptation in single-stranded DNA (ssDNA) and double-stranded DNA (dsDNA) within the moderate-tension regime (6.5–18.0 pN). For ssDNA, applied force primarily suppresses configurational entropy, promotes backbone alignment, and reduces stacking interactions, leading to substantial molecular extension. In contrast, dsDNA accommodates mechanical stress through helical twist relaxation, localized terminal fraying, and modest perturbations of stacking interactions while largely preserving duplex integrity.

3.5 Relative Strain and Mechanical Compliance

The relative strain, Eq. (17) is shown in Fig. 2(d). Consistent with the extension analysis, ssDNA accumulates substantially larger strain than dsDNA across the investigated force range. The increasing separation between the two curves suggests that the mechanical differences between ssDNA and dsDNA become more pronounced as force increases. At low force, both molecules remain relatively close to their equilibrium conformations. By 18 pN, however, the ssDNA chain has undergone extensive conformational reorganization while the duplex remains comparatively resistant to deformation. This divergence may represent one of the clearest indicators that the two systems follow distinct force-accommodation pathways long before the onset of classical overstretching.

3.6 Stacking Rearrangement as an Early Mechanical Response

The force dependence of the stacking fraction is shown in Fig. 3(a). Stacking interactions play a central role in stabilizing both ssDNA and dsDNA, making them particularly informative indicators of structural adaptation. The ssDNA molecule exhibits a pronounced decrease in stacking fraction with increasing force. This decline appears closely linked to the structural transition visible in Fig. 1. As the chain becomes increasingly aligned, neighboring bases are less able to maintain favorable stacked arrangements, resulting in progressive loss of local stabilization. The dsDNA response is considerably weaker. Although some reduction in stacking fraction is evident, the magnitude of the change remains small. Cooperative stabilization provided by the duplex architecture likely buffers stacking interactions against mechanical perturbation. This observation is important because it suggests that stacking disruption occurs much earlier in ssDNA than in dsDNA. Previous studies have often emphasized hydrogen-bond disruption as the dominant marker of structural destabilization. The present results suggest a different picture: within the moderate-force regime, stacking rearrangement may be among the earliest detectable responses.

3.7 Preservation of Duplex Integrity

Base-pair occupancy provides a direct measure of duplex stability and is shown in Fig. 3(b). Across all force conditions, occupancy remains close to unity. The duplex therefore retains nearly complete structural integrity despite increasing tension. This finding confirms that the investigated force range remains well below the threshold required for widespread force-induced melting. A slight downward trend is nevertheless apparent. While modest, this reduction may indicate the onset of localized destabilization. Importantly, the decrease in base-pair occupancy is substantially smaller than the reduction in stacking fraction. The implication is that force perturbs stacking interactions before it significantly disrupts hydrogen bonding. This sequence of events forms one of the more interesting mechanistic outcomes of the study. It suggests that the earliest stages of duplex adaptation

involve subtle redistribution of local interactions rather than immediate loss of Watson–Crick pairing.

3.8 Helical Relaxation and Force Redistribution

Figure 3(c) presents the average helical twist as a function of force. A gradual decrease in twist is observed with increasing tension. The trend suggests that the duplex partially relaxes its helical geometry to accommodate applied stress. Such behavior provides a plausible mechanism through which force can be redistributed without extensive disruption of base pairing. An important feature of the results is that twist relaxation occurs while base-pair occupancy remains high. This indicates that geometric adaptation precedes substantial hydrogen-bond loss. In other words, the duplex first changes shape before it begins to lose structural integrity. The snapshots shown in Fig. 1 are consistent with this interpretation. The overall duplex architecture remains preserved, yet subtle geometric adjustments become visible at higher force levels. These adjustments may reflect precisely the twist-relaxation mechanism captured quantitatively in Fig. 3(c).

3.9 Localized Fraying as the Earliest Destabilization Pathway

The evolution of fraying length is shown in Fig. 3(d). Unlike base-pair occupancy, which remains close to unity, fraying exhibits a systematic increase with force. This result suggests that the duplex does not destabilize uniformly. Instead, structural perturbations emerge preferentially at terminal regions where stability is intrinsically lower. Such behavior is physically reasonable because end base pairs experience fewer stabilizing interactions than those in the duplex interior. The coexistence of increasing fraying length and high base-pair occupancy implies a hierarchical response to force. Localized fluctuations appear first at the termini, while the majority of the duplex remains intact. Only at substantially higher forces would one expect these localized disruptions to propagate into larger-scale structural transitions.

3.10 Coupling between Global Mechanics and Local Structure

The correlation matrix presented in Fig. 4 provides a more integrated perspective. Several trends are immediately apparent. End-to-end distance and radius of gyration exhibit strong positive correlations, indicating that molecular extension is accompanied by global expansion. Persistence length also correlates positively with extension, consistent with force-induced alignment reducing bending fluctuations. By contrast, stacking fraction displays strong negative correlations with extension-related observables. This relationship suggests that mechanical elongation and stacking stabilization compete with one another. As force promotes extension, stacking interactions become progressively less favorable. Base-pair occupancy and helical twist exhibit positive correlations, reflecting their common role in maintaining duplex structure. Fraying length is negatively correlated with both quantities, supporting the interpretation that localized destabilization emerges through terminal

fluctuations. Although correlation does not establish causality, the overall pattern lends support to the mechanistic picture developed throughout the Results section. Global deformation appears intimately linked to local structural adaptation rather than occurring independently of it.

3.11 Mechanistic Synthesis and Novel Insights

Figure 5 summarizes the mechanistic pathways inferred from the simulations. Two distinct modes of force accommodation emerge. For ssDNA, force primarily suppresses configurational entropy, promotes backbone alignment, weakens stacking interactions, and ultimately produces substantial extension. The process is largely global in nature, affecting the overall conformation of the molecule. For dsDNA, the response follows a different route. Applied stress is redistributed through helical twist relaxation, localized terminal fraying, and relatively minor perturbations of stacking interactions while preserving high base-pair occupancy. As a result, extension remains comparatively modest. Fig. 5 further integrates the findings from Figs. 1–4 and highlights the central contribution of the study. Rather than focusing on the well-studied overstretching regime, the present work demonstrates that the divergence between ssDNA and dsDNA mechanics emerges much earlier, within a moderate-force window where both molecules remain structurally intact. This distinction represents the primary novelty of the study. Previous investigations have frequently examined ssDNA and dsDNA separately or concentrated on high-force transitions. Here, both molecular forms were interrogated under identical thermodynamic and mechanical conditions, allowing their force-accommodation pathways to be compared directly. The results suggest that structural adaptation begins through different microscopic mechanisms long before classical overstretching or melting occurs. In ssDNA, entropy suppression and stacking loss dominate. In dsDNA, geometric relaxation and localized fraying absorb mechanical stress while preserving duplex stability. Such differences may have important implications for understanding how nucleic acids respond to the modest forces commonly encountered during biological processes such as replication, transcription, and protein-mediated DNA manipulation.

CONCLUSION

This study employed the oxDNA2 coarse-grained model to investigate and directly compare the force-induced structural responses of single-stranded DNA (ssDNA) and double-stranded DNA (dsDNA) under moderate tensile loading (6.5–18.0 pN) at 300 K and 1 M salt concentration. Unlike many previous studies that focus primarily on equilibrium elasticity or high-force overstretching transitions, the present work examined an intermediate mechanical regime where structural adaptation begins to emerge while overall molecular integrity is largely maintained. By subjecting ssDNA and dsDNA to identical thermodynamic and mechanical conditions, it was possible to isolate the molecular mechanisms through which each system accommodates

externally applied stress. The simulations revealed that ssDNA and dsDNA follow fundamentally different deformation pathways. In ssDNA, increasing force produced substantial conformational expansion, progressive backbone alignment, increasing persistence length, and significant reduction in stacking interactions. These changes collectively indicate that force accommodation is dominated by suppression of configurational entropy and large-scale structural reorganization. The corresponding force–extension response showed markedly higher compliance, reflecting the absence of stabilizing Watson–Crick interactions and the greater conformational freedom of the single strand.

The dsDNA exhibited a contrasting response. Although extension increased with force, the magnitude of deformation remained comparatively modest. Base-pair occupancy remained close to unity throughout the investigated force range, indicating preservation of duplex integrity. At the same time, measurable reductions in helical twist, minor decreases in stacking fraction, and increasing terminal fraying suggested that mechanical stress was redistributed through localized structural adjustments rather than global conformational reorganization. The results imply that twist relaxation and terminal destabilization act as early force-accommodation mechanisms before significant hydrogen-bond disruption occurs. Correlation analysis further demonstrated that global mechanical descriptors and local structural observables are strongly coupled. Molecular extension and radius of gyration were positively correlated, whereas stacking fraction exhibited strong negative correlations with deformation-related metrics. Fraying length was negatively correlated with duplex stability indicators, supporting a hierarchical model in which localized terminal fluctuations precede broader structural perturbations.

The principal contribution of this work lies in demonstrating that the divergence between ssDNA and dsDNA mechanics becomes evident well below the classical overstretching regime. Rather than representing different stages of a common deformation process, the two molecular forms appear to employ distinct molecular strategies for accommodating tensile stress. ssDNA responds primarily through entropy-driven conformational reorganization and stacking loss, whereas dsDNA maintains structural integrity through cooperative stabilization, twist relaxation, and localized fraying. These findings provide a mechanistic bridge between equilibrium elasticity and high-force overstretching studies and offer new insight into how nucleic acids respond to the moderate forces commonly encountered during biological processes such as replication, transcription, recombination, and protein-mediated DNA manipulation. Beyond their biological significance, the results also demonstrate the capability of coarse-grained models to resolve subtle force-induced structural transitions that may be difficult to capture experimentally. Future work could extend the present framework to investigate sequence dependence, temperature–force coupling, salt-mediated effects, and higher-force regimes approaching

overstretching transitions. Such studies may further clarify how molecular architecture governs nucleic-acid mechanics across a broad range of physical and biological environments.

REFERENCES

- Buche, M. R., Silberstein, M. N., & Grutzik, S. J. (2022). Freely jointed chain models with extensible links. *Physical Review E*, 106(2), 024502. [\[Crossref\]](#)
- Bustamante, C., Bryant, Z., & Smith, S. B. (2003). Ten years of tension: Single-molecule DNA mechanics. *Nature*, 421(6921), 423-427. [\[Crossref\]](#)
- Chen, H., Meisburger, S. P., Pabit, S. A., Sutton, J. L., Webb, W. W., & Pollack, L. (2012). Ionic strength-dependent persistence lengths of single-stranded RNA and DNA. *Proceedings of the National Academy of Sciences*, 109(3), 799-804. [\[Crossref\]](#)
- Cluzel, P., Lebrun, A., Heller, C., Lavery, R., Viovy, J. L., Chatenay, D., & Caron, F. (1996). DNA: An extensible molecule. *Science*, 271(5250), 792-794. [\[Crossref\]](#)
- Cocco, S., Marko, J. F., & Monasson, R. (2001). Force and kinetic barriers to unzipping of the DNA double helix. *Proceedings of the National Academy of Sciences*, 98(15), 8608-8613. [\[Crossref\]](#)
- Cocco, S., Yan, J., Léger, J. F., Chatenay, D., & Marko, J. F. (2004). Overstretching and force-driven strand separation of double-helix DNA. *Physical Review E*, 70(1), 011910. [\[Crossref\]](#)
- Dans, P. D., Walther, J., Gómez, H., & Orozco, M. (2016). Multiscale simulation of DNA. *Current Opinion in Structural Biology*, 37, 29-45. [\[Crossref\]](#)
- Doye, J. P. K., Ouldrige, T. E., Louis, A. A., Romano, F., Šulc, P., Matek, C., Snodin, B. E. K., Rovigatti, L., Schreck, J. S., Harrison, R. M., & Smith, W. P. J. (2013). Coarse-graining DNA for simulations of DNA nanotechnology. *Physical Chemistry Chemical Physics*, 15(47), 20395-20414. [\[Crossref\]](#)
- Flyvbjerg, H., & Petersen, H. G. (1989). Error estimates on averages of correlated data. *The Journal of Chemical Physics*, 91(1), 461-466. [\[Crossref\]](#)
- Gore, J., Bryant, Z., Nöllmann, M., Le, M. U., Cozzarelli, N. R., & Bustamante, C. (2006). DNA overwinds when stretched. *Nature*, 442(7104), 836-839. [\[Crossref\]](#)
- Gravina, N. M., Gumbart, J. C., & Kim, H. D. (2021). Coarse-grained simulations of DNA reveal angular dependence of sticky-end binding. *The Journal of Physical Chemistry B*, 125(16), 4016-4024. [\[Crossref\]](#)
- Gross, P., Laurens, N., Oddershede, L. B., Bockelmann, U., Peterman, E. J. G., & Wuite, G. J. L. (2009). Unraveling the structure of a single DNA during overstretching using multicolor fluorescence imaging. *Biophysical Journal*, 96, 291a. [\[Crossref\]](#)
- Harrison, R. M., Romano, F., Ouldrige, T. E., Louis, A. A., & Doye, J. P. K. (2019). Identifying physical causes of apparent enhanced cyclization of short DNA molecules with a coarse-grained model. *Journal of Chemical Theory and Computation*, 15(8), 4660-4672. [\[Crossref\]](#)
- Ke, C., Humeniuk, M., S-Gracz, H., & Marszalek, P. E. (2007). Direct measurements of base stacking interactions in DNA by single-molecule atomic-force spectroscopy. *Physical Review Letters*, 99(1), 018302. [\[Crossref\]](#)
- King, G. A., Gross, P., Bockelmann, U., Modesti, M., Wuite, G. J. L., & Peterman, E. J. G. (2013). Revealing the competition between peeled ssDNA, melting bubbles, and S-DNA during DNA overstretching using fluorescence microscopy. *Proceedings of the National Academy of Sciences*, 110(10), 3859-3864. [\[Crossref\]](#)
- Lankaš, F., Lavery, R., & Maddocks, J. H. (2006). Kinking occurs during molecular dynamics simulations of small DNA minicircles. *Structure*, 14(10), 1527-1534. [\[Crossref\]](#)
- Léger, J. F., Romano, G., Sarkar, A., Robert, J., Bourdieu, L., Chatenay, D., & Marko, J. F. (1999). Structural transitions of a twisted and stretched DNA molecule. *Physical Review Letters*, 83(5), 1066-1069. [\[Crossref\]](#)
- Marin-Gonzalez, A., Vilhena, J. G., Perez, R., & Moreno-Herrero, F. (2017). Understanding the mechanical response of double-stranded DNA and RNA under constant stretching forces using all-atom molecular dynamics. *Proceedings of the National Academy of Sciences*, 114(27), 7049-7054. [\[Crossref\]](#)
- Marko, J. F., & Siggia, E. D. (1994). Bending and twisting elasticity of DNA. *Macromolecules*, 27(4), 981-988. [\[Crossref\]](#)
- Marko, J. F., & Siggia, E. D. (1995a). Statistical mechanics of supercoiled DNA. *Physical Review E*, 52(3), 2912-2938. [\[Crossref\]](#)
- Marko, J. F., & Siggia, E. D. (1995b). Stretching DNA. *Macromolecules*, 28(26), 8759-8770. [\[Crossref\]](#)
- McIntosh, D. B., Duggan, G., Gouil, Q., & Saleh, O. A. (2014). Sequence-dependent elasticity and electrostatics of single-stranded DNA: Signatures of base-stacking. *Biophysical Journal*, 106(3), 659-666. [\[Crossref\]](#)
- Murphy, M. C., Rasnik, I., Cheng, W., Lohman, T. M., & Ha, T. (2004). Probing single-stranded DNA conformational flexibility using fluorescence spectroscopy. *Biophysical Journal*, 86(4), 2530-2537. [\[Crossref\]](#)
- Ouldrige, T. E., Louis, A. A., & Doye, J. P. K. (2011). Structural, mechanical, and thermodynamic properties of a coarse-grained DNA model. *The Journal of Chemical Physics*, 134(8), 085101. [\[Crossref\]](#)
- Paik, D. H., & Perkins, T. T. (2011). Overstretching DNA at 65 pN does not require peeling from free ends or nicks. *Journal of the American Chemical Society*, 133(10), 3219-3221. [\[Crossref\]](#)
- Pérez, A., Lankas, F., Luque, F. J., & Orozco, M. (2008). Towards a molecular dynamics consensus view of B-DNA flexibility. *Nucleic Acids Research*, 36(7), 2379-2394. [\[Crossref\]](#)

- Romano, F., Piana, S., Ouldrige, T. E., Doye, J. P. K., & Louis, A. A. (2013). Coarse-grained simulations of DNA overstretching. *The Journal of Chemical Physics*, 138(8), 085101. [\[Crossref\]](#)
- Saleh, O. A., McIntosh, D. B., Pincus, P., & Ribbeck, N. (2009). Nonlinear low-force elasticity of single-stranded DNA molecules. *Physical Review Letters*, 102(6), 068301. [\[Crossref\]](#)
- Sengar, A., Ouldrige, T. E., Henrich, O., Rovigatti, L., & Šulc, P. (2021). A primer on the oxDNA model of DNA: When to use it, how to simulate it and how to interpret the results. *Frontiers in Molecular Biosciences*, 8, Article 693710. [\[Crossref\]](#)
- Smith, S. B., Cui, Y., & Bustamante, C. (1996). Overstretching B-DNA: The elastic response of individual double-stranded and single-stranded DNA molecules. *Science*, 271(5250), 795-799. [\[Crossref\]](#)
- Snodin, B. E. K., Randisi, F., Mosayebi, M., Šulc, P., Schreck, J. S., Romano, F., Ouldrige, T. E., Tsukanov, R., Nir, E., Louis, A. A., & Doye, J. P. K. (2015). Introducing improved structural properties and salt dependence into a coarse-grained model of DNA. *The Journal of Chemical Physics*, 142(23), 234901. [\[Crossref\]](#)
- Strick, T. R., Allemand, J. F., Bensimon, D., Bensimon, A., & Croquette, V. (2000). Twisting and stretching single DNA molecules. *Progress in Biophysics and Molecular Biology*, 74(1-2), 115-140. [\[Crossref\]](#)
- Šulc, P., Romano, F., Ouldrige, T. E., Doye, J. P. K., & Louis, A. A. (2014). A nucleotide-level coarse-grained model of RNA. *The Journal of Chemical Physics*, 140(23), 235102. [\[Crossref\]](#)
- Šulc, P., Romano, F., Ouldrige, T. E., Rovigatti, L., Doye, J. P. K., & Louis, A. A. (2012). Sequence-dependent thermodynamics of a coarse-grained DNA model. *The Journal of Chemical Physics*, 137(13), 135101. [\[Crossref\]](#)
- Van Mameren, J., Gross, P., Farge, G., Hooijman, P., Modesti, M., Falkenberg, M., Wuite, G. J. L., & Peterman, E. J. G. (2009). Unraveling the structure of DNA during overstretching by using multicolor, single-molecule fluorescence imaging. *Proceedings of the National Academy of Sciences*, 106(43), 18231-18236. [\[Crossref\]](#)
- Wang, M. D., Yin, H., Landick, R., Gelles, J., & Block, S. M. (1997). Stretching DNA with optical tweezers. *Biophysical Journal*, 72(3), 1335-1346. [\[Crossref\]](#)
- Yang, Y., Zhang, X., Li, Y., & others. (2019). Theoretical study of overstretching DNA-RNA hybrid duplex. *Chinese Physics B*, 28, 018701. [\[Crossref\]](#)
- Zhang, Y., Zhou, H., & Ou-Yang, Z. C. (2001). Stretching single-stranded DNA: Interplay of electrostatic, base-pairing, and base-pair stacking interactions. *Biophysical Journal*, 81(2), 1133-1143. [\[Crossref\]](#)